Electromagnetic Wave Interactions with a Metamaterial Cloak

Hongsheng Chen,[1,2,*] Bae-Ian Wu,[2] Baile Zhang,[2] and Jin Au Kong[1,2]

[1]*The Electromagnetics Academy at Zhejiang University, Zhejiang University, Hangzhou 310058, China*

[2]*Research Laboratory of Electronics, Massachusetts Institute of Technology, Cambridge, Massachusetts 02139, USA*

(Received 19 January 2007; published 6 August 2007)

We establish analytically the interactions of electromagnetic wave with a general class of spherical cloaks based on a full wave Mie scattering model. We show that for an ideal cloak the total scattering cross section is absolutely zero, but for a cloak with a specific type of loss, only the backscattering is exactly zero, which indicates the cloak can still be rendered invisible with a monostatic (transmitter and receiver in the same location) detection. Furthermore, we show that for a cloak with imperfect parameters the bistatic (transmitter and receiver in different locations) scattering performance is more sensitive to $\eta_t = \sqrt{\mu_t/\epsilon_t}$ than $n_t = \sqrt{\mu_t\epsilon_t}$.

DOI: 10.1103/PhysRevLett.99.063903 PACS numbers: 42.25.Fx, 41.20.Jb

Recently, invisibility cloaking has received much attention [1–11]. The design process for the cloak is mostly based on a coordinate transformation [4]. An optical conformal mapping method has also been used for the design of a medium that creates perfect invisibility in the ray tracing limit [6]. The design approach in Ref. [4] started from Maxwell's equations, which indicated such cloaking should be effective at all frequencies. Cummer *et al.* demonstrated the full wave cylindrical cloaking but with purely numerical calculations that do not provide as much insight into the physics as an analytical approach [2]. The analytical demonstrations reported so far are mostly in the geometrical optics limit or in the electrostatic or magnetostatic limit [4–6]. Since both of the two limiting cases include approximations in Maxwell's theory, it is very necessary to demonstrate analytically whether perfect invisibility, which can be characterized by a zero cross section, is achievable under any wavelength condition. Furthermore, none of the methods reported in [4–6] provides analytical solutions on how sensitive the nonideal cloaks are to the material perturbations as well as how good the cloaks are in terms of bistatic scattering.

In this Letter, the interactions of electromagnetic wave with the cloaks are analytically established based on a full wave Mie scattering model [12–14]. Since the cloak is both anisotropic and inhomogeneous [4], the Mie scattering theory is extended to be applicable to this special case, and then the analytical expressions of the electromagnetic field in the whole space are rigorously calculated. We show that for an ideal cloak with the parameters specified in Ref. [4], the total scattering cross section is absolutely zero. Furthermore, the performance and sensitivity of the cloak with nonideal parameters are quantitatively calculated and the physics behind the phenomenon are interpreted.

Figure 1 shows that an E_x polarized plane wave with unit amplitude, $E_i = \hat{x}e^{ik_0 z}$, is incident upon the coated sphere along the $\hat{z}$ direction. $k_0 = \omega\sqrt{\mu_0\epsilon_0}$ is the wave number in air. The time dependence of $e^{-i\omega t}$ is suppressed. Without loss of generality, we assume the inner sphere ($r < R_1$) has a permittivity of ϵ_1 and permeability of μ_1. The cloak ($R_1 < r < R_2$) is a kind of rotationally uniaxial media characterized by

$$\bar{\bar{\epsilon}} = [\epsilon_r(r) - \epsilon_t]\hat{r}\,\hat{r} + \epsilon_t\bar{\bar{I}} \qquad \bar{\bar{\mu}} = [\mu_r(r) - \mu_t]\hat{r}\,\hat{r} + \mu_t\bar{\bar{I}}, \tag{1}$$

where $\bar{\bar{I}} = \hat{r}\,\hat{r} + \hat{\theta}\,\hat{\theta} + \hat{\phi}\,\hat{\phi}$, ϵ_t and μ_t are the permittivity and permeability along the $\hat{\theta}$ and $\hat{\phi}$ direction, $\epsilon_r(r)$ and $\mu_r(r)$ are the permittivity and permeability along the $\hat{r}$ direction, and both of them are functions of r. The field expressions for the wave propagation inside the cloak are first studied. For source free cases, we decompose the fields into TE and TM modes (with respect to $\hat{r}$) by introducing the scalar potentials, Φ_{TM} and Φ_{TE}:

$$\begin{aligned} B_{\mathrm{TM}} &= \nabla \times (\hat{r}\Phi_{\mathrm{TM}}), \\ D_{\mathrm{TM}} &= \frac{1}{-i\omega}\{\nabla \times [\bar{\bar{\mu}}^{-1} \cdot \nabla \times (\hat{r}\Phi_{\mathrm{TM}})]\}, \\ B_{\mathrm{TE}} &= \frac{1}{-i\omega}\{\nabla \times [\bar{\bar{\epsilon}}^{-1} \cdot \nabla \times (\hat{r}\Phi_{\mathrm{TE}})]\}, \\ D_{\mathrm{TE}} &= -\nabla \times (\hat{r}\Phi_{\mathrm{TE}}). \end{aligned} \tag{2}$$

Using Eqs. (1) and (2) and after some algebraic manipulations, we can obtain the wave equations for Φ_{TM} and Φ_{TE}:

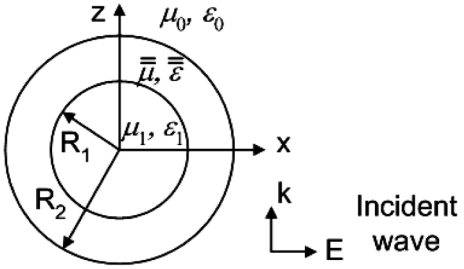

FIG. 1. Configuration of scattering of plane wave by a sphere coated with a cloak.

$$\left\{\frac{1}{(\mathrm{SR})}\frac{\partial^2}{\partial r^2}+\frac{1}{r^2\sin\theta}\frac{\partial}{\partial\theta}\left(\sin\theta\frac{\partial}{\partial\theta}\right)+\frac{1}{r^2\sin^2\theta}\frac{\partial^2}{\partial\phi^2}+\frac{1}{(\mathrm{SR})}k_t^2\right\}\Phi=0, \quad (3)$$

where $k_t=\omega\sqrt{\mu_t\epsilon_t}$; (SR) denotes the anisotropic ratio of the cloak, for TM wave, $(\mathrm{SR})=\epsilon_t/\epsilon_r$, and for TE wave, $(\mathrm{SR})=\mu_t/\mu_r$. Using the separation of variables method and assuming $\Phi=f(r)g(\theta)h(\phi)$, we get $h(\phi)$ as harmonic functions: $h(\phi)=e^{\pm im\phi}$, $g(\theta)$ as associated Legendre polynomials: $g(\theta)=P_n^m(\cos\theta)$, and $f(r)$ as the solution of the following equation:

$$\left\{\frac{\partial^2}{\partial r^2}+\left[k_t^2-(\mathrm{SR})\frac{n(n+1)}{r^2}\right]\right\}f(r)=0. \quad (4)$$

If we take the parameters suggested in [4]: $\epsilon_t=\epsilon_0\frac{R_2}{R_2-R_1}$, $\epsilon_r=\epsilon_t\frac{(r-R_1)^2}{r^2}$, $\mu_t=\mu_0\frac{R_2}{R_2-R_1}$, and $\mu_r=\mu_t\frac{(r-R_1)^2}{r^2}$, then for both TE and TM modes, we get $(\mathrm{SR})=\frac{r^2}{(r-R_1)^2}$. Therefore, the solution of Eq. (4) is

$$f(r)=k_t(r-R_1)b_n(k_t(r-R_1)), \quad (5)$$

where b_n is the spherical Bessel function. From the above analysis, we see that the solutions of Eq. (3) in the cloak layer are composed of a superposition of Bessel functions, associated Legendre polynomials, and harmonic functions.

In order to match the boundary conditions on the spherical surface, the incident fields are expanded in terms of spherical harmonics. With the solutions of Eq. (3) for the cloak layer, we can get the scalar potentials, respectively, for the incident fields ($r>R_2$), the scattered fields ($r>R_2$), the internal fields ($r<R_1$), and the fields of the cloak layer ($R_1<r<R_2$), to be of the form:

$$\begin{aligned}\Phi_{\mathrm{TM}}^i&=\frac{\cos\phi}{\omega}\sum_n a_n\psi_n(k_0r)P_n^1(\cos\theta),\\ \Phi_{\mathrm{TE}}^i&=\frac{\sin\phi}{\omega\eta_0}\sum_n a_n\psi_n(k_0r)P_n^1(\cos\theta),\end{aligned} \quad (6)$$

$$\begin{aligned}\Phi_{\mathrm{TM}}^s&=\frac{\cos\phi}{\omega}\sum_n a_nT_n^{(M)}\zeta_n(k_0r)P_n^1(\cos\theta),\\ \Phi_{\mathrm{TE}}^s&=\frac{\sin\phi}{\omega\eta_0}\sum_n a_nT_n^{(N)}\zeta_n(k_0r)P_n^1(\cos\theta),\end{aligned} \quad (7)$$

$$\begin{aligned}\Phi_{\mathrm{TM}}^{\mathrm{int}}&=\frac{\cos\phi}{\omega}\sum_n c_n^{(M)}\psi_n(k_1r)P_n^1(\cos\theta),\\ \Phi_{\mathrm{TE}}^{\mathrm{int}}&=\frac{\sin\phi}{\omega\eta_0}\sum_n c_n^{(N)}\psi_n(k_1r)P_n^1(\cos\theta),\end{aligned} \quad (8)$$

$$\begin{aligned}\Phi_{\mathrm{TM}}^c&=\frac{\cos\phi}{\omega}\sum_n\{d_n^{(M)}\psi_n(k_t(r-R_1))\\ &\quad+f_n^{(M)}\chi_n(k_t(r-R_1))\}P_n^1(\cos\theta),\\ \Phi_{\mathrm{TE}}^c&=\frac{\sin\phi}{\omega\eta_0}\sum_n\{d_n^{(N)}\psi_n(k_t(r-R_1))\\ &\quad+f_n^{(N)}\chi_n(k_t(r-R_1))\}P_n^1(\cos\theta),\end{aligned} \quad (9)$$

where $a_n=\frac{(-i)^{-n}(2n+1)}{n(n+1)}$, $n=1,2,3,\ldots$, $\eta_0=\sqrt{\mu_0/\epsilon_0}$, $k_1=\omega\sqrt{\mu_1\epsilon_1}$. $T_n^{(M)}$, $T_n^{(N)}$, $d_n^{(M)}$, $d_n^{(N)}$, $f_n^{(M)}$, and $f_n^{(N)}$ are unknown expansion coefficients. $\psi_n(\xi)$, $\chi_n(\xi)$ and $\zeta_n(\xi)$ represent the Riccati-Bessel functions of the first, the second, and the third kind, respectively [15]. Using Eq. (2), the electromagnetic fields in the three regions can be expanded in terms of the corresponding scalar potentials [16]. By applying the boundary conditions at the surface, we can get four equations at $r=R_1$ and four equations at $r=R_2$. Note that there are two equations at $r=R_1$ given by:

$$\frac{\epsilon_t}{\epsilon_1}c_n^{(N)}\psi_n(k_1R_1)=d_n^{(N)}\psi_n(0)+f_n^{(N)}\chi_n(0) \quad (10)$$

$$\frac{\mu_t}{\mu_1}c_n^{(M)}\psi_n(k_1R_1)=d_n^{(M)}\psi_n(0)+f_n^{(M)}\chi_n(0). \quad (11)$$

We see $\psi_n(0)=0$ and $\chi_n(0)$ is an infinite term for all $n\geq 1$. Since the field in the hidden sphere should be finite, $f_n^{(N)}$ and $f_n^{(M)}$ must be kept zero. We see the field in the hidden object is decoupled with those in the other regions. From the other four equations at the boundary of $r=R_2$, we can calculate the following coefficients:

$$T_n^{(M)}=-\frac{\psi_n'(\xi_0)\psi_n(\xi_t)-(\eta_t/\eta_0)\psi_n(\xi_0)\psi_n'(\xi_t)}{\zeta_n'(\xi_0)\psi_n(\xi_t)-(\eta_t/\eta_0)\zeta_n(\xi_0)\psi_n'(\xi_t)} \quad (12)$$

$$T_n^{(N)}=-\frac{\psi_n(\xi_0)\psi_n'(\xi_t)-(\eta_t/\eta_0)\psi_n'(\xi_0)\psi_n(\xi_t)}{\zeta_n(\xi_0)\psi_n'(\xi_t)-(\eta_t/\eta_0)\zeta_n'(\xi_0)\psi_n(\xi_t)} \quad (13)$$

$$d_n^{(M)}=a_n\frac{i\mu_t/\mu_0}{\zeta_n'(\xi_0)\psi_n(\xi_t)-(\eta_t/\eta_0)\zeta_n(\xi_0)\psi_n'(\xi_t)} \quad (14)$$

$$d_n^{(N)}=a_n\frac{i\epsilon_t/\epsilon_0}{\zeta_n'(\xi_0)\psi_n(\xi_t)-(\eta_0/\eta_t)\zeta_n(\xi_0)\psi_n'(\xi_t)}, \quad (15)$$

where $\xi_0=k_0R_2$, $\xi_t=k_t(R_2-R_1)$, and $\eta_t=\sqrt{\mu_t/\epsilon_t}$. If $\epsilon_t=\epsilon_0\frac{R_2}{R_2-R_1}$, $\mu_t=\mu_0\frac{R_2}{R_2-R_1}$, then $\xi_t=\xi_0$, $\eta_t=\eta_0$. Using the Wronskians for the spherical pairs of solutions, the above four equations are simplified to be:

$$T_n^{(M)}=T_n^{(N)}=0, \qquad d_n^{(M)}=\frac{\epsilon_t}{\epsilon_0}a_n, \qquad d_n^{(N)}=\frac{\mu_t}{\mu_0}a_n. \quad (16)$$

It is very interesting to see that the scattering coefficients, $T_n^{(M)}$ and $T_n^{(N)}$, are equal to zero. The exactly zero scattered

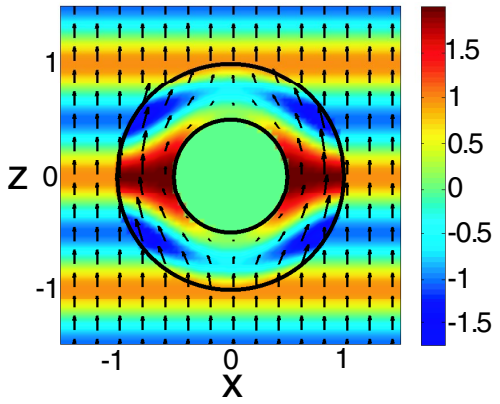

FIG. 2 (color online). E_x field distribution and Poynting vectors due to an E_x polarized plane wave incidence onto an ideal cloak with $R_1 = 0.5\lambda_0$ and $R_2 = \lambda_0$.

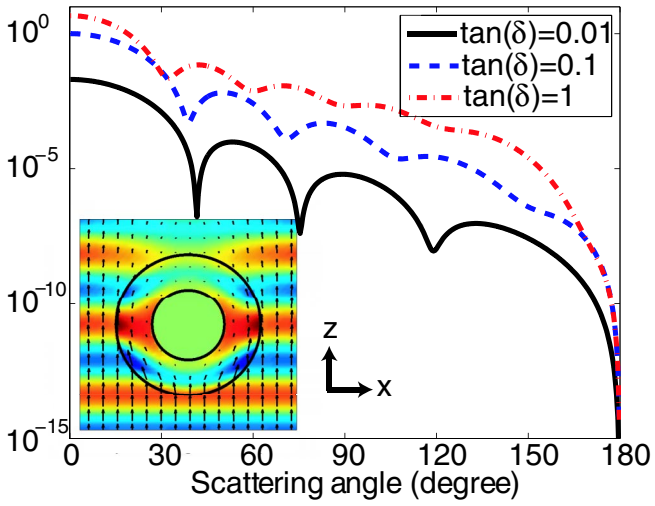

FIG. 3 (color online). Normalized differential cross sections for a cloak ($R_1 = 0.5\lambda_0$, $R_2 = \lambda_0$) with a specified loss tangent introduced in each component of the permittivity and permeability. The inset shows the E_x field for the case of $\tan\delta = 0.1$.

field indicates the reflectionless behavior of the perfect cloak [4]. It should be noted that our mathematical demonstration is applicable to any wavelength condition. Figure 2 shows the calculated electric fields and the Poynting vectors due to an E_x polarized plane wave incidence onto a cloak with $R_1 = 0.5\lambda_0$ and $R_2 = \lambda_0$ (λ_0 denotes the wavelength in free space). We see that the hidden object is completely hide from the waves, corroborating the effectiveness of the cloak proposed in [4]. There is no on-axis ray problem [4] here since the Poynting power becomes zero as the field penetrate deep into the cloak [2].

The most interesting thing is that Eqs. (12)–(15) give further information. For example, it is known that loss is often an important issue. When the electric and magnetic loss tangents are introduced, the scattering coefficients $T_n^{(M)}$ and $T_n^{(N)}$ become nonzero. In Fig. 3, we plot the bistatic scattering as a function of the scattering angle θ for the loss tangent of 0.01, 0.1, and 1, respectively. The vertical axis represents the normalized differential cross sections, $\frac{|S_1(\theta)|^2}{k_0^2\pi R_2^2}$, $\frac{|S_2(\theta)|^2}{k_0^2\pi R_2^2}$, where $S_1(\theta)$ and $S_2(\theta)$ are defined by [12]:

$$S_1(\theta) = -\sum_n \frac{(2n+1)}{n(n+1)}[T_n^{(M)}\pi_n(\theta) + T_n^{(N)}\tau_n(\theta)],$$
$$S_2(\theta) = -\sum_n \frac{(2n+1)}{n(n+1)}[T_n^{(M)}\tau_n(\theta) + T_n^{(N)}\pi_n(\theta)]. \quad (17)$$

In the above two equations $\pi_n(\theta)$ and $\tau_n(\theta)$ are related to the associated Legendre functions by $\pi_n(\theta) = -\frac{P_n^1(\cos\theta)}{\sin\theta}$ and $\tau_n(\theta) = -\frac{dP_n^1(\cos\theta)}{d\theta}$, respectively [15]. For the configuration shown in Fig. 1, $S_1(\theta)$ and $S_2(\theta)$ represent the scattering patterns in the yz and xz planes, respectively. The two curves of $S_1(\theta)$ and $S_2(\theta)$ overlap because $T_n^{(M)} = T_n^{(N)}$. From Fig. 3 we see that the scattered power increases as the loss increases. A more interesting phenomenon is that the backscattering magnitude is always zero [because $T_n^{(M)} = T_n^{(N)}$, and $\pi_n(\theta) = -\tau_n(\theta)|_{\theta=180^\circ}$], which is very different from conventional scattering from regular particles [12]. The calculated field distribution in the xz plane for the spherical cloak with $\tan\delta = 0.1$ (Fig. 3, inset) is similar to the simulation results of a cylindrical cloak with the same type of loss [2]. However, our analytical calculation shows that only the spherical cloak in this particular lossy case exhibits exactly zero backscattering. This unique property of the spherical cloak indicates the cloaked object can still completely hide from a monostatic radar detection.

Since the constitutive parameters for a perfect cloak are very difficult to realize, nonideal material parameters are more often used in the measurements [1,2]. Hence, it is worthwhile to study how the imperfect material parameters quantitatively affect the performance of the cloak. We calculate the normalized scattering cross section $Q_{\text{sca}} = \frac{2}{(k_0R_2)^2}\sum_n(2n+1)(|T_n^{(M)}|^2 + |T_n^{(N)}|^2)$ as ϵ_t changes under three cases: (Case I) keep $\mu_t = \mu_0\frac{R_2}{R_2-R_1}$ constant; (Case II) keep the impedance $\eta_t = \sqrt{\mu_t/\epsilon_t} = \eta_0$ constant; and (Case III) keep the refractive index $n_t = \sqrt{\frac{\mu_t\epsilon_t}{\mu_0\epsilon_0}} = \frac{R_2}{R_2-R_1}$ constant. The results are shown in Fig. 4(a), where the horizontal axis ϵ_t is normalized by the ideal parameter $\epsilon_0\frac{R_2}{R_2-R_1}$. We see that when ϵ_t is equal to the ideal parameter, the corresponding μ_t in the three cases are all equal to $\mu_0\frac{R_2}{R_2-R_1}$, and Q_{sca} is equal to 0, meaning the cloak is perfect. When ϵ_t slightly changed from the ideal parameter, Q_{sca} in Case I and Case II increase from zero more rapidly than that in Case III. This is because in Case III, the refractive index is kept constant, and the direction of Poynting vector inside the cloak is mostly close to the

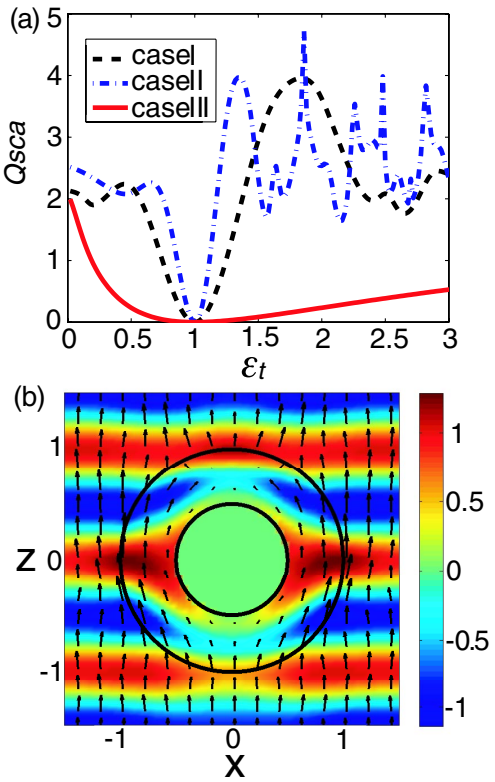

FIG. 4 (color online). (a) Normalized scattering cross section of a cloak as functions of ϵ_t for three different cases: (Case I) keep $\mu_t = \mu_0 \frac{R_2}{R_2 - R_1}$ constant; (Case II) keep $\eta_t = \eta_0$ constant; and (Case III) keep $n_t = \frac{R_2}{R_2 - R_1}$ constant. (b) E_x field distribution and Poynting vectors for Case III with $\epsilon_t = 2\epsilon_0 \frac{R_2}{R_2 - R_1}$ and $\mu_t = \frac{1}{2}\mu_0 \frac{R_2}{R_2 - R_1}$.

ideal case, as shown in Fig. 4(b). Therefore, we can conclude that the bistatic scattering performance of the cloak is more sensitive to $\eta_t = \sqrt{\mu_t/\epsilon_t}$ than $n_t = \sqrt{\mu_t \epsilon_t}$. However, it should be noted that from Eqs. (12), (13), and (17) the cloak in Case II is still invisible with monostatic detection since the matched impedance results in a zero backscattering.

It is important to note that all the above analyses are valid independent of the material parameters of the hidden object. Even when the material parameters of the cloak are imperfect, the incident fields still cannot penetrate into the hidden object, and the scattered power is totally introduced by the cloak itself. This unusual phenomenon is based on the assumption that the material parameters of the cloak in the radial and transverse axis always have the same form of $\kappa_r = \kappa_t \frac{(r-R_1)^2}{r^2}$, where κ represents μ or ϵ. Hence, Eqs. (5), (10), and (11) always hold, leading to $f_n^{(N)} = 0$ and $f_n^{(M)} = 0$, and the material parameters in the hidden object give no contribution to the outside field. If some perturbations are introduced in the relationship of the radial and transverse material parameters, the solution of Eqs. (4) should be revisited, and the interaction of the outside field with the hidden object cannot be omitted.

In conclusion, we have demonstrated the interactions of the electromagnetic wave with the cloaks by rigorously solving Maxwell equations in the spherical coordinate system. The fields and bistatic scattering cross section of a general class of cloaks (ideal and nonideal) have been quantitatively solved by the full wave scattering method. The physics behind the invisibility of the cloak has been interpreted. Our method was shown to be computational efficient, which is very useful for cloak design and applications.

This work was supported by the Chinese NSF under Grant No. 60531020, the China PSF under Grant No. 20060390331, and the ONR under Contract No. N00014-01-1-0713.

*Corresponding author.
chenhs@ewt.mit.edu

[1] D. Schurig *et al.*, Science **314**, 977 (2006).
[2] S. A. Cummer *et al.*, Phys. Rev. E **74**, 036621 (2006).
[3] A. Alu and N. Engheta, Phys. Rev. E **72**, 016623 (2005).
[4] J. B. Pendry, D. Schurig, and D. R. Smith, Science **312**, 1780 (2006).
[5] D. Schurig, J. B. Pendry, and D. R. Smith, Opt. Express **14**, 9794 (2006).
[6] U. Leonhardt, Science **312**, 1777 (2006).
[7] U. Leonhardt, New J. Phys. **8**, 118 (2006).
[8] A. Hendi, J. Henn, and U. Leonhardt, Phys. Rev. Lett. **97**, 073902 (2006).
[9] A. H. Sihvola, Prog. Electromagn. Res. **pier-66**, 191 (2006).
[10] G. W. Milton, M. Briane, and J. R. Willis, New J. Phys. **8**, 248 (2006).
[11] D. A. B. Miller, Opt. Express **14**, 12 457 (2006).
[12] L. Tsang, J. A. Kong, and K. Ding, *Scattering of Electromagnetic Waves: Theories and applications* (Wiley, New York, 2000).
[13] J. A. Kong, *Electromagnetic Waves Theory* (EMW Publishing, Cambridge, MA, 2005).
[14] B. A. Kemp, T. M. Grzegorczyk, and J. A. Kong, Phys. Rev. Lett. **97**, 133902 (2006).
[15] H. C. van de Hulst, *Light Scattering by Small Particles* (Dover, New York, 1957).
[16] J. Roth and M. J. Digman, J. Opt. Soc. Am. **63**, 308 (1973).